Available online at www.sciencedirect.com
ScienceDirect
Catalysis Today 126 (2007) 235–247
CATALYSIS TODAY
www.elsevier.com/locate/cattod

Adsorption of methanol as a probe for surface characteristics of zirconia-, alumina-, and zirconia/alumina-supported chromia catalysts

Satu T. Korhonen [a,*], Miguel A. Bañares [b], José L.G. Fierro [b], A. Outi I. Krause [a]

[a] *Helsinki University of Technology, Department of Chemical Technology, P.O. Box 6100, FI-02015 TKK, Finland*
[b] *Instituto de Catalisis y Petroleoquimica, CSIC, Campus Cantoblanco, E-28049 Madrid, Spain*

Available online 17 January 2007

Abstract

The aim of our study was to improve the supported chromia dehydrogenation catalysts by combining the beneficial properties of the industrially used chromia/alumina (CrAl) catalyst with those of the more active chromia/zirconia (CrZr) catalysts. We report here the results on the surface characteristics, the surface composition and the type of the functional surface species, of chromia/zirconia/alumina (CrZrAl) catalysts that were studied by methanol adsorption–desorption. The measurements were carried out using in situ diffuse reflectance infrared Fourier transform spectroscopy (DRIFTS) and *operando* Raman spectroscopy. The performance of CrZrAl catalysts was compared with CrZr and CrAl catalysts. The CrZrAl catalysts resembled more the CrAl catalysts than the CrZr catalysts in their behavior. Lewis acidity of the alumina support was detected even with the highest used Zr loading of approximately one monolayer. The similar performance of the CrZrAl and the CrAl catalysts was assigned to a strong interaction between zirconia and alumina. Cr on the catalysts activated methanol at low temperatures to form formates, induced basic properties and promoted hydrogen formation.

Keywords: Infrared; Raman; Methanol adsorption; Chromia; Zirconia; Alumina

1. Introduction

The dehydrogenation of light alkanes with chromia/alumina (CrAl) catalysts is an important industrial route for the production of light alkenes from a relatively cheap feedstock [1]. However, according to De Rossi et al. [2] zirconia-supported chromia catalysts (CrZr) are more active in the dehydrogenation reaction. On both supports under oxidizing conditions the main Cr species are Cr^{6+} and Cr^{3+} but some Cr^{5+} species may also exist. The amount of these species depends on the catalyst preparation and pretreatment conditions and the Cr content [1,3]. The monolayer coverage of Cr on alumina is approximately 4–5 at_{Cr}/nm^2 [1,4,5]. Under the dehydrogenation conditions Cr^{6+} and Cr^{5+} reduce to Cr^{3+}. The exposed surface Cr^{3+} ions are the active species in dehydrogenation [1,3]. De Rossi et al. [2] assigned the higher dehydrogenation activity of the CrZr catalysts in comparison to the CrAl catalysts to either a favorable interaction between the zirconia support and the Cr species, or to the existence of a higher concentration of Cr^{5+} species on the zirconia support that reduce to form Cr^{3+} species with higher activity than those present on the alumina surface.

The drawback of zirconia as a support material is, however, its low surface area compared with alumina. To tackle this problem zirconia has been deposited on higher surface area materials, e.g. alumina [6–11] and silica [7,8], for several applications. The deposition of zirconia has mainly been performed by impregnation from solution [6,8–11], but atomic layer deposition (ALD) [7], where the oxide precursors are introduced to the surface from the gas phase, has also been used. The estimates on the value of a monolayer of zirconia on silica or alumina range from 4–5 at_{Zr}/nm^2 [7] to 7.4 at_{Zr}/nm^2 reported for alumina [8,9]. Below the monolayer coverage zirconia is most often assumed to be amorphous while at higher loadings nano-sized tetragonal zirconia crystallites or islands of these crystallites are formed [7,8,10]. Zirconia has also been suspected to migrate into the alumina matrix especially at low loadings [8,9,11].

The aim of this study was to improve the CrZr dehydrogenation catalysts even further by using high surface area zirconia/alumina (ZrAl) supports. The surface characteristics of the Cr

* Corresponding author.
E-mail address: satu.korhonen@tkk.fi (S.T. Korhonen).

0920-5861/$ – see front matter © 2007 Elsevier B.V. All rights reserved.
doi:10.1016/j.cattod.2007.01.008

catalysts (CrZrAl) were studied by methanol adsorption–desorption (AD) in comparison to the CrZr and the CrAl catalysts. We chose to use methanol as the probe molecule because of its ability to simultaneously give information on both the surface composition and type of the functional surface species. By adsorbing a monolayer of methanol to the catalyst surface and by the use of vibrational spectroscopic techniques the catalyst surface can be characterized based on the specific vibrations of the formed methoxy species, i.e. chemisorbed methanol. Furthermore, the functional surface species can be identified by monitoring gaseous products formed. According to Wang and Wachs [12] the formation of carbon dioxide, formaldehyde (HCOH), and dimethylether (DME) are indicators for the presence of basic, redox, and Lewis acid sites, respectively. The optimal conditions for obtaining a monolayer of chemisorbed methanol on metal oxide surfaces are according to Briand et al. [13] the adsorption temperature of 100 °C and the use of dilute methanol feed, i.e. 2000 ppm methanol.

In the present study the surface species and the gaseous products were monitored by in situ diffuse reflectance infrared Fourier transform spectroscopy (DRIFTS) and *operando* Raman spectroscopy in combination with on-line product analysis by mass spectrometry (MS). The use of both DRIFTS and Raman spectroscopy was chosen since they give complementary information on the surface characteristics: DRIFTS is more sensitive towards the adsorbed surface species containing oxygen–hydrogen and carbon–hydrogen bonds while Raman spectroscopy is more sensitive towards the metal–oxygen bonds and sp^2 carbon species.

2. Experimental

2.1. Sample preparation and characterization

The commercial support materials zirconia (Mel Chemicals EC 0100 1/8 in) and alumina (Akzo 000-1.5 E, γ-alumina) were calcined before use at 600 °C for 16 h in air. The high surface area ZrAl supports were prepared by depositing zirconia on alumina by ALD from the gas phase through saturating gas–solid reactions. In these the precursor reacts with the hydroxyl groups of the support to produce a complex still containing some of the precursor ligands. Zirconium chloride ($ZrCl_4$, Fluka 98%) was used as the precursor for zirconia. The formed surface Cl complexes were decomposed to form the oxide by treatment with water at elevated temperatures. The sequences of complex formation and ligand removal were repeated to increase the concentration of the oxide. Two ZrAl supports were prepared containing Zr below or above the monolayer coverage of 4 at_{Zr}/nm^2. These supports were prepared using one or five sequences. The ALD preparation technique for the deposition of zirconia is described in more detail elsewhere [7]. The ZrAl supports were calcined in air at 600 °C for 16 h.

ALD was also used to deposit Cr on the commercial zirconia and alumina supports and on the ALD-prepared ZrAl supports. The ALD preparation technique for the deposition of Cr is similar to that used with zirconia, and is described in more detail elsewhere [14]. Chromium(III) acetylacetonate ($Cr(acac)_3$, Reidel-de Haën 99%) was used as the precursor. The acac ligands were removed by oxygen treatment at elevated temperatures. For the Cr deposition one or two sequences of complex formation and ligand removal were used to prepare in total six different catalysts with Cr loadings below the monolayer coverage of 4 at_{Cr}/nm^2. The Cr catalysts were calcined in air at 600 °C for 4 h before use. The supports and the Cr catalysts are summarized in Table 1.

The surface area and the porosity of the catalysts were determined by BET method at −196 °C using liquid nitrogen as the coolant. The catalyst samples were slowly heated from room temperature to 350 °C after which the samples were degassed at this temperature until the pressure inside the sample holder was 3×10^{-6} Torr or lower. The degassing time was between 30 and 60 min depending on the amount of the sample. The amount of Zr and Cr was determined by X-ray fluorescence (XRF). X-ray photoelectron spectroscopy (XPS) was used to study the surface composition of the ALD-prepared catalysts and the supports.

2.2. In situ DRIFTS measurements

In situ DRIFTS was used to characterize the calcined catalysts and supports and the surface species formed during methanol adsorption. The in situ DRIFTS equipment consisted of a Nicolet Nexus Fourier transform infrared spectrometer and a Spectra-Tech high temperature and high pressure reaction

Table 1
The supports and the catalyst and their characteristics determined by BET and XRF techniques

Sample	Description	SA (m^2/g)	wt% Cr	at_{Cr}/nm^2	wt% Zr	at_{Zr}/nm^2
Al_2O_3	Alumina	185	–	–	–	–
ZrO_2	Zirconia	47	–	–	n.a.[a]	n.a.[a]
4.4ZrAl	Zirconia/alumina	165	–	–	4.4	1.8
15ZrAl [7]	Zirconia/alumina	150	–	–	15	6.7
0.4CrZr	Chromia/zirconia	47	0.4	1.0	–	–
0.8CrZr	Chromia/zirconia	48	0.8	1.9	–	–
1.2CrAl	Chromia/alumina	189	1.2	0.7	–	–
2.2CrAl	Chromia/alumina	181	2.2	1.4	–	–
2.0(4.4)CrZrAl	Chromia/zirconia/alumina	169	2.0	1.4	4.4	1.8
2.1(15)CrZrAl	Chromia/zirconia/alumina	148	2.1	1.6	15	6.7

[a] n.a.: not analyzed.

chamber, combined with a Pfeiffer Vacuums Omnistar MS. All samples were calcined in situ in the reaction chamber for 2 h with 10% O_2/N_2 at 580 °C and reoxidized after the experiments with 2–10% O_2/N_2 at the same temperature. In all experiments the spectrum measured with an aluminium mirror (4 cm^{-1}, 200 scans) was used as the background, and the total gas flow was kept constant at 50 ml/min. Methanol (2000 ppm in N_2, AGA) adsorption experiments were performed to elucidate the surface characteristics of the catalysts. The adsorption experiments were performed either as (i) an adsorption at 100 °C with consequent heating in N_2 flow up to 580 °C (adsorption–desorption, AD), or by (ii) temperature-dependent (TD) measurements. The product gases were monitored on-line by MS during the TD experiments.

The AD experiment at 100 °C was started by directing the methanol-containing gas to the chamber for 25 min. The spectra were recorded every minute (4 cm^{-1}, 30 scans) for the first 10 min and every 5 min (4 cm^{-1}, 100 scans) for the rest of the adsorption. After 25 min on methanol feed the chamber was flushed with N_2 for 5 min after which a spectrum (4 cm^{-1}, 100 scans) was measured under N_2. Thereafter the temperature was increased stepwise to 580 °C under N_2 flow to study the desorption of the surface species. During the desorption phase the spectra were recorded every 25 °C (4 cm^{-1}, 100 scans). The TD measurements were performed by heating the sample stepwise under the methanol feed from room temperature to 100 °C while the spectra were recorded every 25 °C (4 cm^{-1}, 100 scans). At 100 °C the reaction chamber was flushed with N_2 for 5 min to remove gaseous methanol and to study the desorption of the surface species. After the flush a spectrum was measured under N_2 (4 cm^{-1}, 100 scans). Thereafter the methanol feed was redirected to the reaction chamber and the temperature was increased again. The sequence was repeated by measuring the spectra under methanol every 25 °C and under N_2 at 200, 300, 400, 500, and 580 °C.

2.3. Operando *Raman-MS measurements*

The *operando* Raman measurements were performed to characterize the calcined catalysts and supports and to study the methanol adsorption. The *operando* Raman-MS measurements were performed with a Renishaw Micro-Raman System-1000 using a home-made quartz flow-through reactor (*operando* reactor [15]) and a MS for online product analysis. The Raman spectrometer consisted of an Ar^+ (514 nm) laser, a cooled CCD detector and a holographic super-Notch filter for the removal of elastic scattering. The catalyst sample was loaded to the reactor between two layers of silicon carbide to minimize the void volume inside the reactor. The whole system was kept at its place inside the reactor by quartz wool. The catalyst samples were calcined using 5% O_2/He for 2 h at 570 °C after which the reactor was flushed with He for 1 h before the experiments. The methanol adsorption experiments were performed by adsorbing methanol (2000 ppm in He) at 100 °C to the catalysts until the level of methanol observed in the product gas by MS was stabilized to the level of the feed gas. After the adsorption the reactor was flushed with He and heated stepwise to 350 °C. The spectra were recorded under He at 100, 150, 200, 250, 300, and 350 °C.

3. Results

3.1. Characterization of the catalysts and supports

3.1.1. Characterization by BET, XRF, and XPS

The alumina, the zirconia, and the ALD-prepared ZrAl supports and the Cr catalysts were characterized by BET and XRF techniques (Table 1). The samples will be referred to as $x(y)$CrZ, where x is the amount of Cr in wt%, y is the amount of Zr on the alumina support in wt%, and Z is the support, either Zr for zirconia, Al for alumina, or ZrAl for zirconia/alumina. The deposition of zirconia on alumina increased the surface area of the zirconia-based catalysts to over three-fold from the 47 m^2/g of the commercial zirconia support to the 165 m^2/g of the 4.4ZrAl support. All ALD-prepared samples, except the 15ZrAl support, had the same surface area as their parent supports within the ±10% accuracy of the surface area determination method.

The amount of deposited Cr was selected to be comparable for the catalysts with different specific surface areas and is, therefore, presented also as at_{Cr}/nm^2 in Table 1. These values were calculated using the analyzed amounts of Cr in wt% and the determined specific surface areas of the samples. The amount of Cr on the prepared catalysts was below the monolayer coverage of ~4 at_{Cr}/nm^2 [1,4,5] while the amount of zirconium on the prepared supports was either below, or above the value of the monolayer coverage of ~4 at_{Zr}/nm^2 [7].

The alumina, the zirconia, and the 4.4ZrAl supports and the Cr-containing catalysts were also characterized by XPS to further study their surface composition. Table 2 presents the binding energies detected by XPS and the different atomic ratios of the detected elements. The observed binding energies for the Al 2p and the Zr $3d_{5/2}$ photoelectrons for the ALD-prepared catalysts

Table 2
XPS binding energies and atomic ratios for the ALD-prepared catalysts, and the zirconia and the alumina supports

Sample	Al 2p	Zr $3d_{5/2}$	Cr $2p_{3/2}$	Zr/Al	Cr/(Zr + Al)
Al_2O_3	74.5	–	–	–	–
ZrO_2	–	182.2	–	–	–
4.4ZrAl	74.4	182.2	–	0.620	–
2.0(4.4)CrZrAl	74.5	182.2	577.3 (10%)[a] 579.9 (90%)[b]	0.333	0.068
2.1(15)CrZrAl	74.5	182.3	577.6 (33%)[a] 580.0 (67%)[b]	1.05	0.066
0.4CrZr	–	182.2	577.3 (100%)[a]	–	0.035[c]
0.8CrZr	–	182.3	577.3 (39%)[a] 579.5 (61%)[b]	–	0.072[c]
1.2CrAl	74.4	–	577.4 (37%)[a] 580.0 (63%)[b]	–	0.030[d]

[a] Fraction of Cr^{3+} in percentage.
[b] Fraction of Cr^{6+} in percentage.
[c] Cr/Zr.
[d] Cr/Al.

are in accordance with literature values [8,11] for alumina and zirconia, respectively, and with those for the analyzed commercial supports. The decrease in the Zr/Al ratio caused by the deposition of Cr on the 4.4ZrAl support indicated that Cr would preferentially cover Zr rather than Al. The higher binding energy (~580 eV) of the Cr $2p_{3/2}$ corresponds to the Cr^{6+} species and the lower (~577 eV) to the Cr^{3+} species [16]. The absence of the Cr^{6+} signal for the 0.4CrZr catalyst might be due to the detection limit of the XPS for the catalyst with a low surface area and low concentration of Cr. The Cr/Zr, Cr/Al, and Cr/(Zr + Al) ratios were equal for the catalysts prepared by the same number of Cr sequences, i.e. one or two, by ALD in agreement with the calculated surface concentrations (at_{Cr}/nm^2 in Table 1).

3.1.2. Characterization by Raman spectroscopy

The Raman spectra for the calcined catalysts were recorded to investigate the phase of the zirconia and the nature of the Cr species. Fig. 1 presents the Raman spectra for the calcined 0.4CrZr, the 2.1(15)CrZrAl, and the 1.2CrAl catalysts. The bands below 600 cm^{-1} in the spectrum for the 0.4CrZr catalyst are characteristic for the monoclinic phase of zirconia [17] with main bands at 613, 467, and 329 cm^{-1}. This agrees with XRD results performed earlier, which also indicated that the commercial zirconia was monoclinic [18]. For the 1.2CrAl and the 2.1(15)CrZrAl catalysts this region showed the features of the quartz reactor. No bands arising from crystalline zirconia were observed for the ZrAl-supported catalysts even after subtracting the spectrum of the quartz window (Fig. 1).

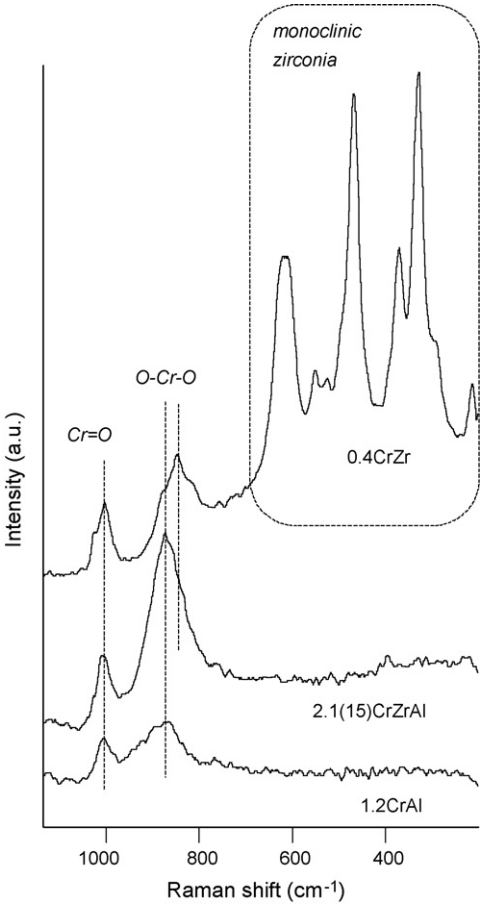

Fig. 1. Raman spectra for the calcined 0.4CrZr, the 2.1(15)CrZrAl, and the 1.2CrAl catalysts. The spectrum of the quartz window has been subtracted from the spectra.

Chromate bands were observed for the 0.4CrZr catalyst at 1012, 875, and 850 cm^{-1}. They were assigned to ν(Cr=O), ν(O–Cr–O), and ν(O–Cr–O) vibrations, respectively, of two different kinds of polymeric Cr species which have different O–Cr–O bond distances and, therefore, show two ν(O–Cr–O) bands in the spectrum [4]. For the 0.8CrZr catalyst the chromate bands were observed at 1026, 1006, 848, and 818 cm^{-1} (not shown). These bands, assigned to ν_{as}(Cr=O), ν_s(Cr=O), ν_{as}(O–Cr–O), and ν_s(O–Cr–O) [4] vibrations, respectively, arise from only one type of polymeric Cr species. This indicates that at higher Cr loading the surface was covered with longer polymeric chains. For the 2.1(15)CrZrAl catalyst the chromate bands were observed at 1012 (ν(Cr=O)) and 875 cm^{-1} (ν(O–Cr–O)), indicating the presence of only one type of polymeric Cr species. The ν(Cr=O) and ν(O–Cr–O) bands were also be observed for the 1.2CrAl catalyst at 1012 and 875 cm^{-1}, respectively. The Raman band at 550 cm^{-1} [19] characteristic for crystalline chromia (Cr_2O_3) was not observed for any of the catalysts.

3.1.3. Characterization by DRIFTS

The DRIFT spectra of the calcined catalysts were recorded to investigate the hydroxyl groups and the Cr species on the catalysts. All calcined Cr-containing catalysts and supports were analyzed by DRIFTS. Fig. 2 presents the DRIFT spectra of CrZr catalysts after calcination. Hydroxyl bands were observed for the calcined zirconia at 3774, 3738, 3675, and a broad feature around 3457 cm^{-1}. These bands were assigned to terminal, bibridged, and terminal hydroxyl groups and to the hydrogen-bonded hydroxyls [20], respectively. The high intensities of the terminal and tribridged hydroxyl bands indicate that the commercial zirconia is monoclinic in accordance with the XRD and Raman results. For the CrZr catalysts the intensity of the hydroxyl bands, especially the terminal hydroxyls, decreased with increasing Cr loading. This is in agreement with the gas–solid reaction mechanism occurring during the ALD preparation where the Cr precursor reacts with the support hydroxyls [14].

Fig. 3 presents the DRIFT spectra for the calcined CrZrAl catalysts, and those for the alumina and the 4.4ZrAl supports as a comparison. For alumina hydroxyls were observed at 3772, 3728, 3685, and a broad feature at 3598 cm^{-1}. These were assigned to terminal, bibridged, tribridged, and hydrogen-bonded hydroxyls [21], respectively. With increasing Cr loading the bands of the hydroxyls on alumina also decreased in intensity, but both terminal and tribridged hydroxyls were consumed (not shown). The hydroxyl bands for the ZrAl samples resembled more the spectrum of alumina than the hydroxyls detected for the monoclinic zirconia. The band observed at 3779 cm^{-1} for the 2.0(4.4)CrZrAl and the 2.1(15)CrZrAl catalysts is suspected to originate from terminal hydroxyls bound to Zr in accordance to the findings of Kytökivi et al. [7], or from terminal hydroxyl groups on alumina shifted

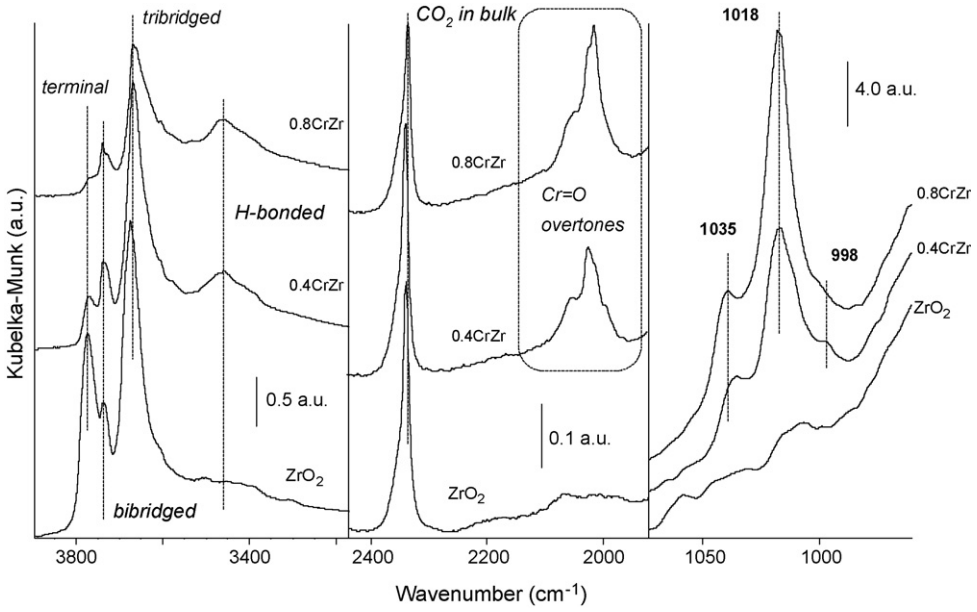

Fig. 2. DRIFT spectra for the calcined zirconia support and the CrZr catalysts.

due to the presence of Cr on the surface. The strong band observed for all samples at 2340 cm^{-1} is assigned to carbon dioxide impurities inside the support [22].

The chromates were observed for all of the Cr-containing catalysts from the overtone bands around 2000 cm^{-1} while for the zirconia-supported samples also the ν(Cr=O) bands could be observed around 1000 cm^{-1} (Fig. 2). The chromates for the 0.4CrZr catalyst were observed at 2049, 2024, 2011, and 1992 cm^{-1} (overtones) as well as at 1035, 1017, and 998 cm^{-1}. These bands most likely arise from the ν_{as}(Cr=O) and ν_{s}(Cr=O) [4] vibrations of polymeric surface chromates. The complexity of these bands is in accordance with the conclusion drawn from

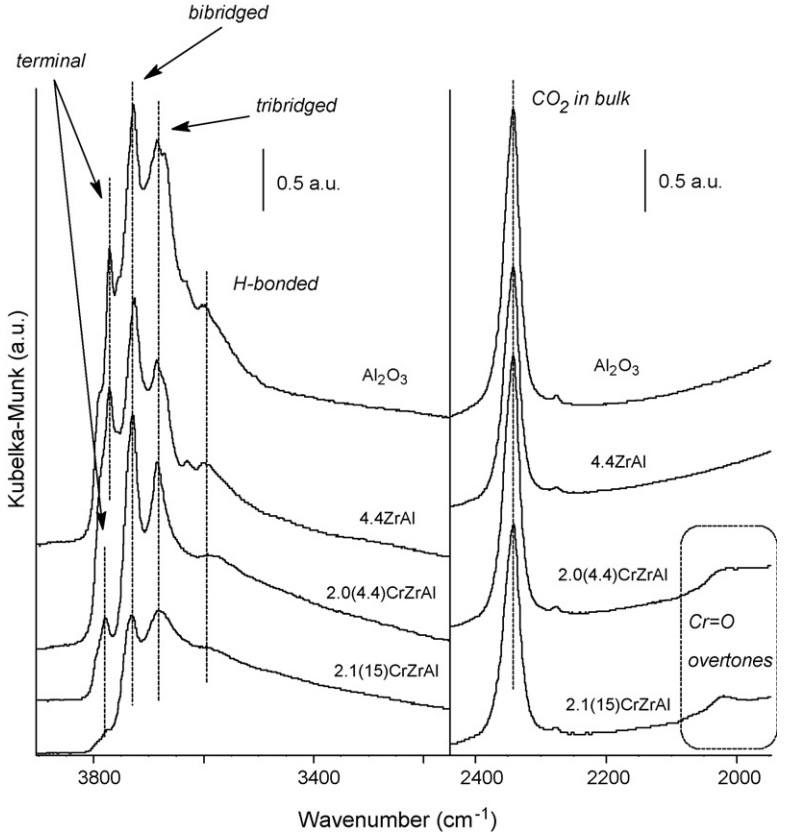

Fig. 3. DRIFT spectra for the CrZrAl catalysts and the 4.4ZrAl and the alumina supports.

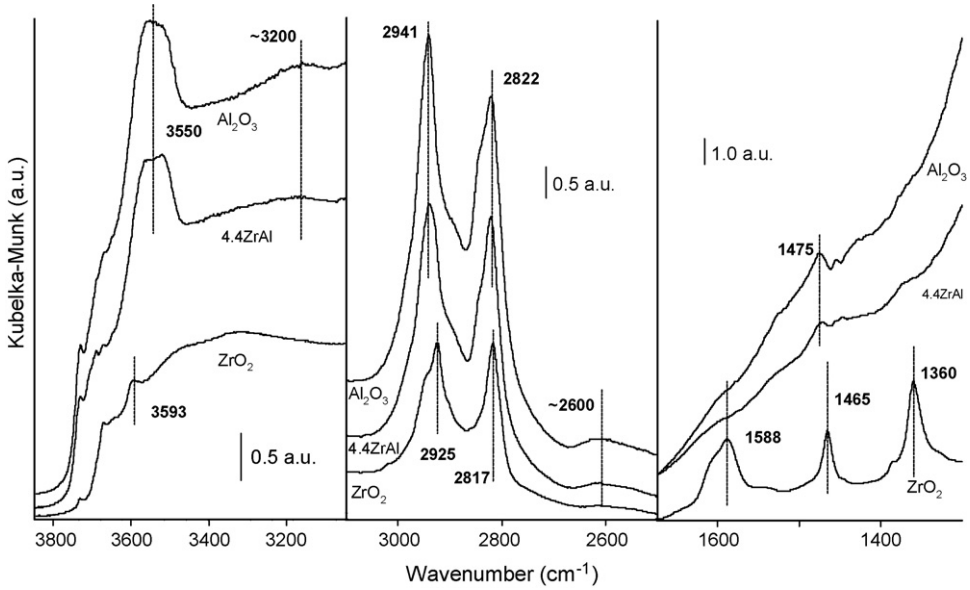

Fig. 4. Comparison of the different supports under methanol (20 min at 100 °C). Spectra recorded with in situ DRIFTS.

the Raman spectra that at least two kinds of polymeric Cr species coexist on the zirconia surface with low Cr loadings. For the 0.8CrZr catalyst the chromates were observed at 2049, 2024, and 2016 cm^{-1} (overtones), and at 1039 and 1018 cm^{-1}. The presence of only two bands originating from the ν(Cr=O) vibrations is in accordance with the Raman results and with the conclusion that with increasing Cr loading only one type of polymeric chromate is present on the surface.

3.2. In situ DRIFTS results on methanol adsorption–desorption (AD)

The in situ DRIFTS methanol AD experiments were performed for all supports and catalysts to study their surface composition. Methanol can adsorb on the catalyst surface either molecularly, i.e. as physisorbed methanol, or dissociatively through chemisorption. The optimal temperature for the formation of a monolayer of chemisorbed methanol is 100 °C when using 2000 ppm methanol [13]. The surface composition of a catalyst is revealed by the vibrations of the methoxy species, i.e. chemisorbed methanol, that are bound to different atoms on the catalyst surface. According to McInroy et al. [23] molecular methanol for η-alumina can be observed by infrared from the bands at ca. 3200 ν(OH), 2940 $\nu_{as}(CH_3)$, 2820 $\nu_s(CH_3)$, and 1460 cm^{-1} $\delta(CH_3)$, of which especially the broad and intense feature around 3200 cm^{-1} is uniquely associated with molecular methanol. The bands originating from the methoxy species for alumina can be observed according to them from the species at 2938 $\nu_{as}(CH_3)$, 2820 $\nu_s(CH_3)$, and 1450 cm^{-1} $\delta(CH_3)$ as well as from the band at 2600 cm^{-1} which is a combination band of the methyl rock at 1170 cm^{-1} and methyl deformation modes at 1460 cm^{-1}. Jung and Bell reported [20] the bands of molecular methanol for monoclinic zirconia to be at 2939 and 2834 cm^{-1} ($\nu_{as}(CH_3)$ and $\nu_s(CH_3)$, respectively) while the methoxy groups can be observed at 2923 and 2816 cm^{-1} ($\nu_{as}(CH_3)$ and $\nu_s(CH_3)$, respectively). The methoxy species for zirconia can also be observed from the $\nu(OCH_3)$ vibrations at 1163 and 1070 cm^{-1} of the on-top and bridging, respectively, methoxy groups on Zr^{4+} [24].

A comparison of the features observed for the alumina, the zirconia, and the 4.4ZrAl supports at 100 °C after 20 min of methanol adsorption is presented in Fig. 4. In common for all samples the hydroxyl groups were consumed during the adsorption along with the formation of water and the methoxy species. For the alumina and the 4.4ZrAl supports Al-bound methoxy species were detected at 2941 and 2940 cm^{-1}, respectively ($\nu_{as}(CH_3)$). The strong $\nu_s(CH_3)$ vibration of molecular methanol at 2822 cm^{-1} prevented the detection of the $\nu_s(CH_3)$ vibration of the methoxy species for the alumina-containing supports at this temperature. The presence of molecular methanol for the alumina-containing supports was confirmed by the broad feature at 3200 cm^{-1}. The methoxy bands were observed for zirconia at 2925 cm^{-1} $\nu_{as}(CH_3)$ and 2817 cm^{-1} $\nu_s(CH_3)$. The $\nu(OCH_3)$ vibrations of on-top and bridging methoxy species were observed at 1162 and 1069 cm^{-1}, respectively (not shown). The presence of molecular methanol was not as obvious for zirconia but a shoulder on the $\nu_{as}(CH_3)$ band could be detected at 2950 cm^{-1} which possibly originates from molecular methanol. The methyl deformation band was observed at 1475 cm^{-1} for the alumina-containing supports and at 1465 cm^{-1} for the zirconia support. The monoclinic zirconia was the only support to show some additional reactivity towards methanol at 100 °C. The formation of formates could be observed from the bands at 1588 cm^{-1} $\nu_{as}(COO)$, 1384 cm^{-1} $\delta(CH)$, and 1360 cm^{-1} $\nu_s(COO)$ [24,25].

After the adsorption all samples were flushed with N_2 and heated stepwise to 580 °C to study the desorption of the carbonaceous species. Fig. 5 presents the spectra for the

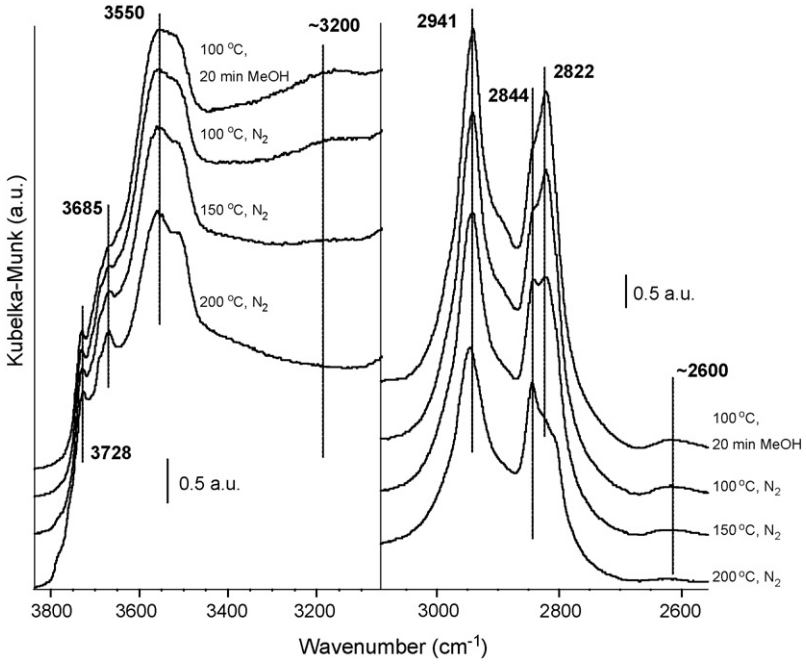

Fig. 5. DRIFT spectra from the methanol desorption (100–200 °C) for the alumina support.

alumina support between 100 and 200 °C. For all alumina-containing supports the disappearance of the 3200 and 2822 cm^{-1} bands indicated that molecular methanol desorbed while heating the samples to 200 °C. Simultaneously, the $\nu_s(CH_3)$ vibration of Al-bound methoxies became visible at 2844 cm^{-1}. No other changes were observed for the alumina-containing supports in this temperature range but for the zirconia support the formate bands grew in intensity. Formates were first observed for the alumina-containing supports around 250 °C.

The bands of molecular methanol were lower in intensity for the Cr-containing catalysts at 100 °C and the different methoxy bands were, therefore, better resolved. The chromates reduced as the methanol-containing gas was directed to the reaction chamber. For the CrZr catalysts methoxy species bound to Cr and Zr were detected. For the alumina-containing catalysts the presence of different methoxy species depended on the Cr and Zr loadings. For the 2.0(4.4)CrZrAl catalyst the methoxy species bound to Al and Zr were observed while for the 2.1(15)CrZrAl catalyst the detected methoxy species were those bound to Cr and Zr. For the alumina-supported catalysts the Cr-bound methoxies were only detected for the 2.2CrAl catalyst. The assignments of the observed bands at 100 °C after 20 min under methanol are presented in Table 3. For all Cr-containing catalysts formates were observed at 100 °C and the intensity of the bands was higher than for the zirconia support.

Fig. 6 presents a comparison of the DRIFT spectra in the CH-region recorded during the desorption of methanol for the Cr-containing catalysts. The spectra labeled with 100 °C were recorded under N_2 after the methanol adsorption. The presence of Al and Zr bound methoxy species for the 2.0(4.4)CrZrAl catalyst and Cr and Zr bound methoxies for the 2.1(15)CrZrAl catalyst could also be observed at 100 °C. Formate bands were observed in the CH-region around 2885 cm^{-1} ν(CH) and 2750 cm^{-1} ($\nu_s(COO) + \delta(CH)$) [24–26] for the Cr-containing catalysts. During the desorption between 100 and 400 °C the formate bands grew in intensity while the methoxy species gradually disappeared. At 400 °C the spectra in the OH-region resembled those of the fresh catalysts. After this temperature the formates also started to disappear. A band around 2960 cm^{-1} was observed for all of the Cr-containing catalysts at higher temperatures and was assigned to the formation of some carbonaceous residues [27].

Table 3
Summary of the bands observed by in situ DRIFTS for molecular methanol and methoxy species (20 min and 100 °C) for the Cr-containing catalysts

Catalyst	Molecular methanol		Methoxy species	
1.2CrAl	ν(OH)	3200	$\nu_{as}(CH_3)$	2944 (Al)
	$\nu_s(CH_3)$	2828	$\nu_s(CH_3)$	2842 (Al), sh[a]
	Combination	2619	$\nu(OCH_3)$I	–
	$\delta(CH_3)$	1472	$\nu(OCH_3)$II	–
2.2CrAl	ν(OH)	3200	$\nu_{as}(CH_3)$	2952 (Cr)
	$\nu_{as}(CH_3)$	2827, sh[a]	$\nu_s(CH_3)$	2843 (Al)
	Combination	2618	$\nu(OCH_3)$I	–
	$\delta(CH_3)$	1470	$\nu(OCH_3)$II	–
0.8CrZr	ν(OH)	3200	$\nu_{as}(CH_3)$	2956 (Cr), 2931 (Zr)
	$\nu_s(CH_3)$	–	$\nu_s(CH_3)$	2852 (Cr), 2830 (Zr)
	Combination	2612	$\nu(OCH_3)$I	1144
	$\delta(CH_3)$	1463	$\nu(OCH_3)$II	1055
2.0(4.4)CrZrAl	ν(OH)	3200	$\nu_{as}(CH_3)$	2948 (Al), 2932 (Zr)
	$\nu_s(CH_3)$	–	$\nu_s(CH_3)$	2844 (Al), 2830 (Zr)
	Combination	2613	$\nu(OCH_3)$I	–
	$\delta(CH_3)$	1471	$\nu(OCH_3)$II	–
2.1(15)CrZrAl	ν(OH)	3200	$\nu_{as}(CH_3)$	2952 (Cr), 2933 (Zr)
	$\nu_s(CH_3)$	–	$\nu_s(CH_3)$	2854 (Cr), 2830 (Zr)
	Combination	2611	$\nu(OCH_3)$I	–
	$\delta(CH_3)$	1460	$\nu(OCH_3)$II	–

[a] sh: shoulder.

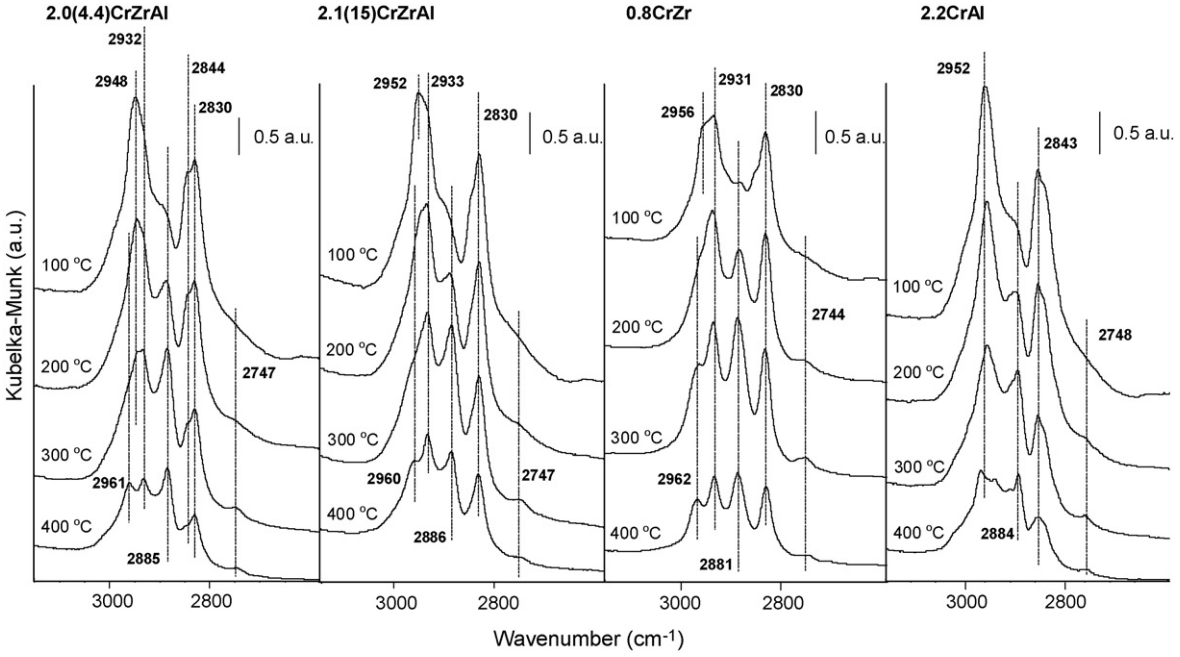

Fig. 6. Comparison of methoxy species observed by in situ DRIFTS for the different Cr-containing catalysts during the methanol desorption.

3.3. Operando *Raman-MS results on methanol adsorption–desorption (AD)*

The methanol AD experiments were also performed with *operando* Raman-MS where by using a flow-through reactor the product distribution could be measured simultaneously with the Raman spectra giving information on both the surface composition and the reactivity. Figs. 7 and 8 present the *operando* Raman-MS spectra recorded during the AD experiment for the 2.1(15)CrZrAl catalyst. The Raman spectra (Fig. 7) showed the formation of Zr- and Cr-bound methoxy species and of formates. Al-bound methoxies were not observed in agreement with the DRIFTS AD results. The broad feature at 1596 cm^{-1} may originate from some coke-like carbonaceous species or aliphatic residues [28,29]. The chromates reduced upon the introduction of methanol at 100 °C as was observed in the in situ DRIFTS AD experiments.

Methanol, HCOH, water, DME, and hydrogen were observed by MS during the heating of the catalyst to 150 °C in He after the adsorption (Fig. 8). These species were the main products up to 250 °C where the formation of carbon dioxide started. Above 250 °C the other gas-phase products were hydrogen and small amounts of DME. The formation of methanol could either originate from the reverse reaction of the methoxy species, from the desorption of molecular methanol, or form a Cannizzaro-like reaction [30]. Both the DRIFT and the Raman spectra, however, indicated that the methoxy species were rather stable at this temperature whereas the presence of molecular methanol was observed in the DRIFT spectra. It is, therefore, suggested that most of the observed methanol in the product gas originated from the molecular methanol present on the catalyst surface at 100 °C. The formation of HCOH was assigned by Wang and Wachs [12] to the redox properties of the catalyst surface and it is, therefore, assigned by us to the presence of Cr on our catalyst. According to Wang and Wachs [12] the formation of carbon dioxide and DME are indicative of the basic and Lewis acidic, respectively, properties of the surface. The low carbon-content of the gaseous products below 250 °C is in accordance with the stability of the formates and methoxy species observed in the DRIFT and the Raman spectra. Above this temperature the Raman spectra indicated that the carbonaceous surface species desorbed.

3.4. *In situ DRIFTS results on methanol temperature-dependent (TD) experiments*

The in situ TD experiments were performed to extend the temperature range of the methanol adsorption experiments. The results of the methanol TD experiment for the 2.1(15)CrZrAl catalyst are presented in Figs. 9 and 10. Similar surface species were detected in the TD experiments below 400 °C as in the in situ and *operando* AD measurements. The formates disappeared from the spectra for the monoclinic zirconia support and for the CrZr catalysts above 400 °C similar to the in situ AD experiments. Starting from this temperature new bands were formed at 1529, 1434, and 1351 cm^{-1} that were assigned to carboxylate-type species. The bands are tentatively assigned to the $\nu_{as}(COO)$, $\nu_s(COO)$, and $\delta(CH_3)$ vibrations, respectively, of acetate species [25]. The formation of the carboxylate species for the alumina-containing catalysts was detected from the broadening of the formate band around 1580 cm^{-1} and the formation of the $\nu_s(COO)$ and $\delta(CH_3)$ bands, but these were less intense than for the zirconia-supported catalysts or even for the monoclinic zirconia support.

The gaseous products were monitored by MS during the TD measurements (Fig. 10). Between 100 and 200 °C the detected

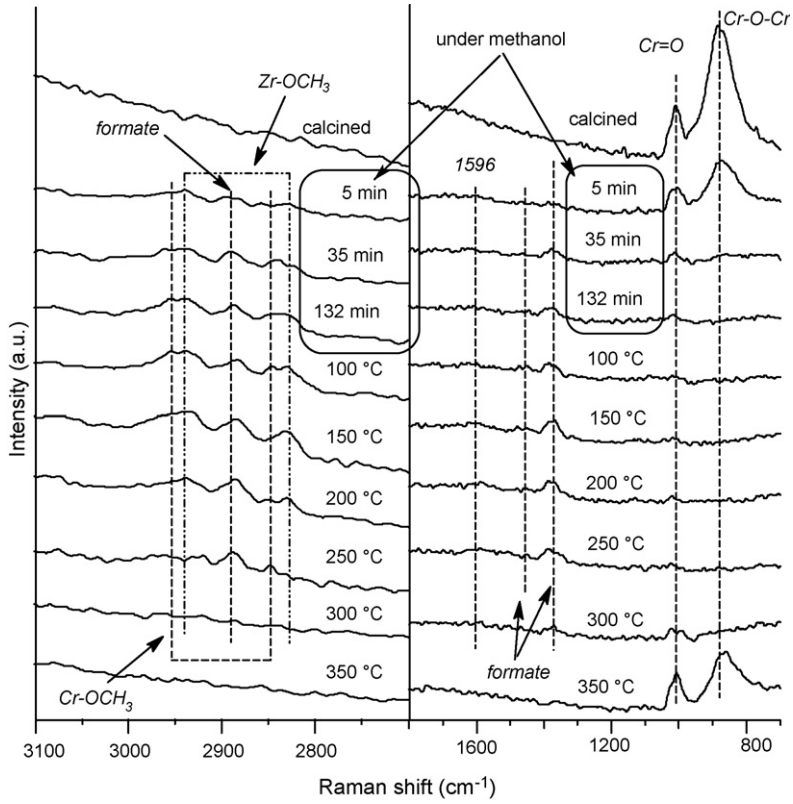

Fig. 7. Raman spectra from the methanol AD experiment for the 2.1(15)CrZrAl catalyst.

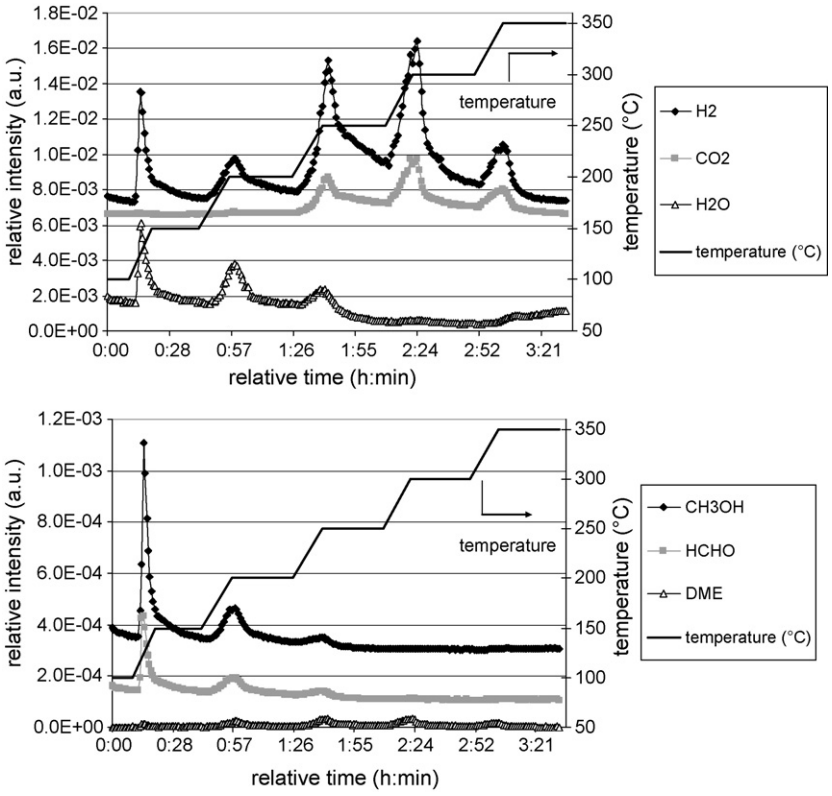

Fig. 8. MS results from the *operando* Raman methanol AD experiment for the 2.1(15)CrZrAl catalyst. The MS results for hydrogen (H_2), carbon dioxide (CO_2), methanol (CH_3OH), and formaldehyde (HCOH) have been shifted upwards to allow the inspection of all products in detail.

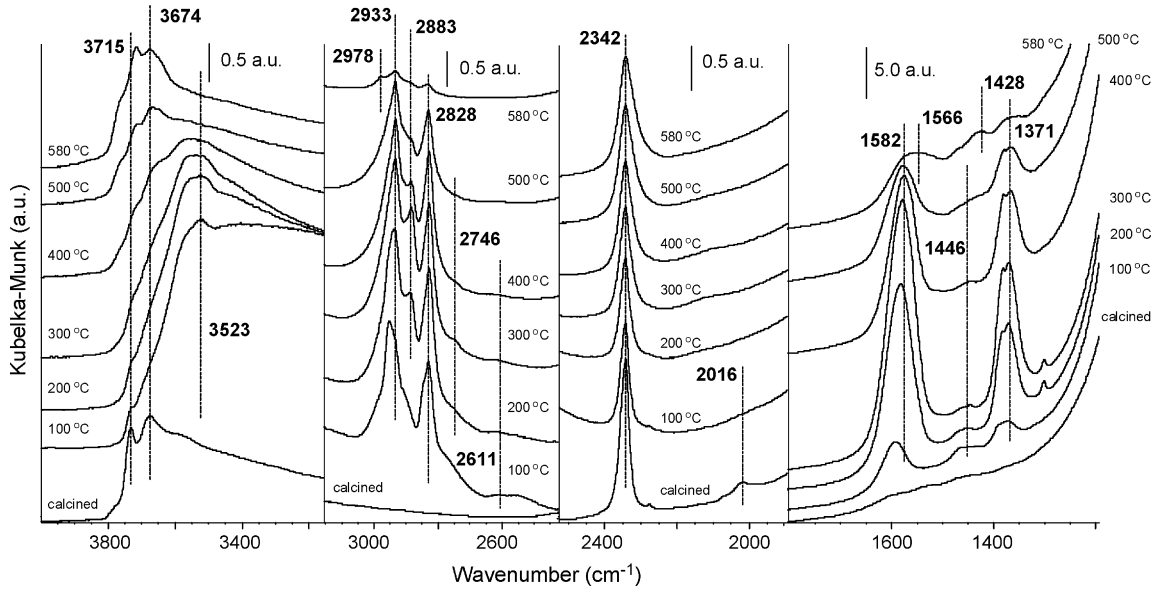

Fig. 9. The in situ DRIFT spectra from the methanol TD experiment for the 2.1(15)CrZrAl catalyst.

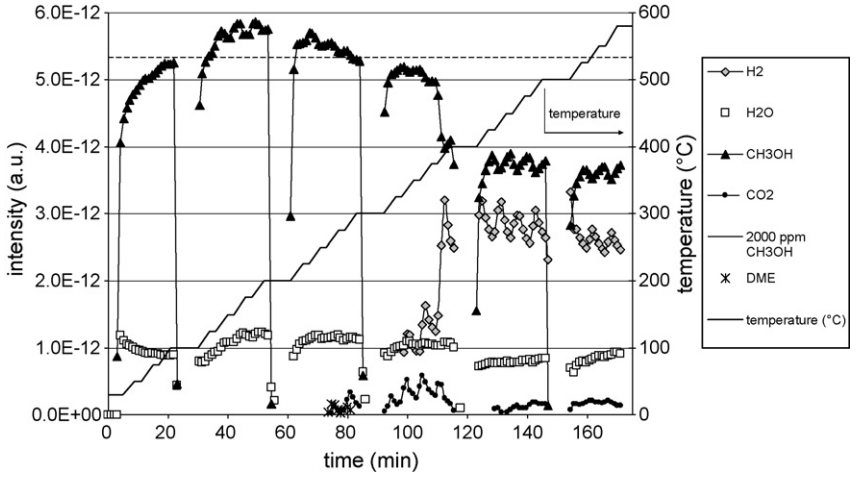

Fig. 10. The MS results from the in situ DRIFTS TD experiment for the 2.1(15)CrZrAl catalyst.

level of methanol in the product gas exceeded that of the feed for all samples indicating that molecular methanol desorbed. Table 4 presents the temperature ranges for the formation of DME, carbon dioxide, and hydrogen for the alumina and the zirconia supports and the 1.2CrAl, the 2.1(15)CrZrAl, and the 0.8CrZr catalysts. The formation of DME was observed for all alumina-containing catalysts, but the temperature range depended on the catalyst. For the alumina support DME formed already around 150 °C, whereas for the CrAl and the CrZrAl catalysts it was first observed around 200 and 250 °C, respectively. The formation of carbon dioxide, indicative of surface basicity, was observed for all catalysts and supports except for the zirconia support, but again the temperature of formation depended on the catalyst. For the Cr-containing catalysts carbon dioxide was observed to form around 250–300 °C. The amount of carbon dioxide was, however, lowest for the CrZr catalysts. For the alumina support carbon dioxide was not observed until 450 °C while for the zirconia support its formation was not detected under our experimental conditions. The formation of hydrogen was observed for all samples, but again the temperature of its formation depended on the sample.

Table 4
The temperature ranges (°C) for the formation of DME, CO_2, and H_2 in the TP experiments

Sample	DME	CO_2	H_2
Al_2O_3	150–300	450–500	450–580 (300–580)[a]
ZrO_2	–	–	450–580 (250–580[a]
1.2CrAl	200–300	300–400 (250–580)[a]	325–580
2.1(15)CrZrAl	250–300	300–400 (250–580)[a]	325–580
0.8CrZr	–	(300–580)[a]	325–580

[a] The temperatures in the parentheses indicate the whole temperature range of formation while the values in front of them indicate the temperature range where the formation was strongest.

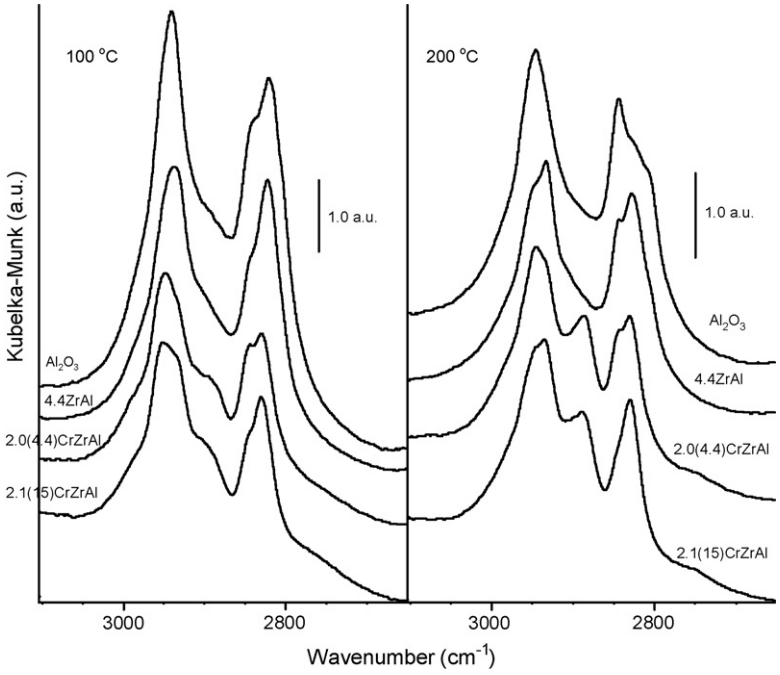

Fig. 11. Summary on methoxy species observed by in situ DRIFTS for the CrZrAl catalysts. The spectra of the alumina and the 4.4ZrAl supports are presented as comparison.

For the Cr-containing catalysts hydrogen was observed to form at 325 °C. The formation of hydrogen was observed for the zirconia and the alumina supports around 250 and 300 °C, respectively.

4. Discussion

Methanol adsorption–desorption (AD) and temperature-dependent (TD) experiments were used to study the surface properties and compositions of ZrAl-, alumina-, and zirconia-supported Cr catalysts. For all catalysts carbonaceous surface species accumulated on the surface below 250 °C and desorbed mainly above this temperature. The detected carbonaceous surface species for all catalysts were the methoxy species and formates, and especially for the alumina-containing samples molecular methanol was also observed at 100 °C. Due to the presence of molecular methanol (Figs. 4 and 5), the conditions presented by Briand et al. [13] for the formation of a monolayer of chemisorbed methanol do not appear optimal for the alumina-containing catalysts reported here. However, the presence of molecular methanol at 100 °C had little effect on the performance of the catalysts since they behaved similar in all experiments at higher temperatures.

Fig. 11 presents a summary on the bands detected by in situ DRIFTS in the CH-region for the CrZrAl catalysts at 100 and 200 °C during the methanol desorption. At 100 °C molecular methanol was observed for the alumina-containing supports whereas for the 2.0(4.4)CrZrAl catalyst Al- and Zr-bound methoxies and for the 2.1(15)CrZrAl catalyst Cr- and Zr-bound methoxies were detected. At 200 °C most of the molecular methanol had desorbed revealing both Zr- and Al-bound methoxies for the 4.4ZrAl support. The intensities of the Zr-bound methoxies were lower than the intensities of the Al-bound species for the 4.4ZrAl support and the 2.0(4.4)CrZrAl catalyst. No clear indication for the presence of Al-bound methoxies was detected for the 2.1(15)CrZrAl catalyst. The results, therefore, suggest that 15 wt% Zr is enough to either cover the alumina surface, or to hinder alumina from reacting with methanol. The XPS results (Table 2) showed equal amounts of Zr and Al on the surface of the 2.1(15)CrZrAl catalyst. The probe depth of XPS is, however, few atomic layers. This could be due to either a surface with equal amounts of both atoms, or an alumina surface fully covered by a thin layer of zirconia. It is however, more likely that the surface composition is something between these extremes, particularly a thin zirconia layer in close interaction with the alumina support.

It has been suggested that by depositing zirconia on alumina at low loadings either an amorphous layer of zirconia is formed [7], or that Zr atoms migrate into the alumina surface forming a mixed $ZrAl_4O_8$ oxide [8,9,11]. With increasing loadings crystalline tetragonal zirconia is formed [8]. No crystalline zirconia was observed for our ZrAl samples even with the Zr loading of near one monolayer (Fig. 1). Our XPS results (Table 2) showed that the ZrAl samples had the same Zr $3d_{5/2}$ binding energy as bulk zirconia. Faro et al. [9,11] and Damyanova et al. [8] reported that a higher value may indicate the migration of Zr into alumina. Our XPS results, therefore, do not indicate the presence of a mixed oxide. The DRIFT spectra for the calcined samples (Figs. 2 and 3), however, showed that the hydroxyl species for the ZrAl samples were similar to those for the alumina support. Also the methanol adsorption experiments showed that the ZrAl samples behaved more like the alumina-supported ones than the ones containing

monoclinic zirconia. Our results, therefore, indicate that there is of a strong interaction between alumina and zirconia, but that they do not form a mixed oxide.

In the *operando* AD and the in situ TD experiments the product gases were monitored on-line by MS. DME was observed for all alumina-containing catalysts and supports. All of the alumina-containing catalysts were, therefore, Lewis acidic, but the deposition of Cr and Zr either consumed the most acidic Al^{3+} species, or modified them. The strongest Lewis acid sites were on the alumina support, where DME was first observed at the lowest temperature, and the weakest on the CrZrAl catalysts, where DME was formed at the highest temperature. For a catalytic application, where the replacement of alumina by zirconia as support material has beneficial effect on the performance of the catalyst, the surface of the ZrAl support should resemble more zirconia than alumina. Therefore, even higher loadings of Zr might be needed to suppress the strong interaction between alumina and zirconia. However, the surface area (Table 1) of the ZrAl support decreases with increasing Zr loading gradually canceling the beneficial effect on the surface area.

Carbon dioxide formed for all samples except the zirconia support. The deposition of Cr on the supports lowered the formation temperature of carbon dioxide. The highest concentration of carbon dioxide was observed starting from approximately 300 °C. This is approximately the temperature, which we have previously reported to be the reduction temperature of the chromates when using isobutane as feed gas for zirconia-supported [18] and alumina-supported [31] catalysts. Some of the carbon dioxide was most likely formed when the chromates reduced but it is also suggested that Cr increased the basicity of both the alumina and the zirconia supports. Cr deposition also affected the formation of hydrogen. Hydrogen formation was observed for all Cr-containing catalysts above 325 °C. This could indicate that hydrogen is formed on the Cr^{3+} species that are active in the dehydrogenation reaction. Hydrogen formation was also observed for the supports, indicating that at least some part of it was formed in reactions not involving the Cr^{3+} species. However, the amount of produced hydrogen was lower with the supports than with the Cr-containing catalysts. The formation of hydrogen on the supports is suggested to be related to the decomposition of the formates that has been reported to be at least a minor route in the water gas shift reaction for zirconia-supported [32,33], ceria-supported [33,34], and zirconia/ceria-supported [33] Pt catalysts.

5. Conclusions

The surface characteristics and reactivity of the ZrAl-, zirconia-, and alumina-supported Cr catalysts were studied by methanol AD and TD experiments using both in situ DRIFTS and *operando* Raman spectroscopy. The ZrAl-supported catalysts resembled the alumina-supported ones in their properties, rather than the zirconia-supported catalysts. Lewis acidic surface species were detected on all alumina-containing samples. The results did not fully support the suggested formation of a mixed oxide through Zr migration into alumina, but clearly indicated a strong interaction between them. Methoxy species bound to Zr and Al were detected for the ZrAl samples with low Zr loading while Cr- and Zr-bound methoxy species were observed for the high loading catalyst 2.1(15)CrZrAl. The role of Cr on the catalysts was to activate methanol to form formates at low temperatures and to produce hydrogen and carbon dioxide at higher temperatures. The formation of carbon dioxide revealed that the deposition of Cr induced basic surface species on all the studied supports while the formation of Cr^{3+} species active in the dehydrogenation reaction was suspected to account for the hydrogen formation.

Acknowledgements

The authors gratefully acknowledge the financial support provided by the Academy of Finland and the Spanish Ministry of Education and Science (CTQ2005-02802/PPQ), and the aid provided by the European coordination action CONCORDE in organizing the researcher exchange between Helsinki University of Technology and the CSIC. The authors express their gratitude to Dr. Sanna Airaksinen for valuable discussions. The authors thank Dr. Arja Kytökivi, Mr. Olli Jylhä, and Ms. Heli Vuori for their help in the preparation of the catalysts, Dr. Anna Lewandowska for her help with the *operando* measurements and Ms. Susanna Wallenius for carrying out some of the in situ DRIFTS experiments.

References

[1] B.M. Weckhuysen, R.A. Schoonheydt, Catal. Today 51 (1999) 223.
[2] S. De Rossi, M.P. Casaletto, G. Ferraris, A. Cimino, G. Minelli, Appl. Catal. A 167 (1998) 257.
[3] R.L. Puurunen, B.M. Weckhuysen, J. Catal. 210 (2002) 418.
[4] M.A. Vuurman, I.E. Wachs, D.J. Stufkens, A. Oskam, J. Mol. Catal. 80 (1993) 209.
[5] M. Cherian, M.S. Rao, W.-T. Yang, J.-M. Jehng, A.M. Hirt, G. Deo, Appl. Catal. A 233 (2002) 21.
[6] A.B. Gaspar, L.C. Dieguez, J. Catal. 220 (2003) 309.
[7] A. Kytökivi, E.-L. Lakomaa, A. Root, H. Österholm, J.-P. Jacobs, H.H. Brongersma, Langmuir 13 (1997) 2717.
[8] S. Damyanova, P. Grange, B. Delmon, J. Catal. 168 (1997) 421.
[9] A.C. Faro Jr., K.R. Souza, J.G. Eon, A.A. Leitão, A.B. Rocha, R.B. Capaz, Phys. Chem. Chem. Phys. 5 (2003) 3811.
[10] M.M.V.M. Souza, D.A.G. Arando, M. Schmal, J. Catal. 204 (2001) 498.
[11] A.C. Faro Jr., K.R. Souza, V.L.D.L. Camorim, M.B. Cardoso, Phys. Chem. Chem. Phys. 5 (2003) 1932.
[12] X. Wang, I.E. Wachs, Catal. Today 96 (2004) 211.
[13] L.E. Briand, A.M. Hirt, I.E. Wachs, J. Catal. 202 (2001) 268.
[14] A. Hakuli, A. Kytökivi, A.O.I. Krause, Appl. Catal. A 190 (2000) 219.
[15] M.O. Guerrero-Pérez, M.A. Bañares, Catal. Today 113 (2006) 48.
[16] B. Liu, M. Terano, J. Mol. Catal. A 172 (2001) 227.
[17] C.L. Pieck, M.A. Bañares, M.A. Vicente, J.L.G. Fierro, Chem. Mater. 13 (2001) 1174.
[18] S.T. Korhonen, S.M.K. Airaksinen, A.O.I. Krause, Catal. Today 112 (2006) 37.
[19] T.V.M. Rao, G. Deo, J.-M. Jehng, I.E. Wachs, Langmuir 20 (2004) 7159.
[20] K.T. Jung, A.T. Bell, Top. Catal. 20 (2002) 97.
[21] C. Morterra, G. Magnacca, Catal. Today 27 (1996) 497.
[22] E. Guglieminotti, Langmuir 6 (1990) 1455.

[23] A.R. McInroy, D.T. Lundie, J.M. Winfield, C.C. Dudman, P. Jones, D. Lennon, Langmuir 20 (2005) 11092.
[24] E. Finocchio, M. Daturi, C. Binet, J.C. Lavalley, G. Blanchard, Catal. Today 52 (1999) 53.
[25] E. Finocchio, G. Busca, V. Lorenzelli, R.J. Willey, J. Catal. 151 (1995) 204.
[26] G. Busca, J. Lamotte, J.-C. Lavalley, V. Lorenzelli, J. Am. Chem. Soc. 109 (1987) 5197.
[27] D.H. William, I. Flemming, Spectroscopic Methods in Organic Chemistry, McGraw-Hill Publishing Company Limited, London, 1966, pp. 52–54.
[28] S. Kuba, H. Knözinger, J. Raman Spectrosc. 33 (2002) 325.
[29] G. Mul, M.A. Bañares, G.G. Cortéz, B. van der Linden, S.J. Khatib, J.A. Moulijn, Phys. Chem. Chem. Phys. 5 (2003) 4378.
[30] G. Busca, A.S. Elmi, P. Forzatti, J. Phys. Chem. 91 (1987) 5263.
[31] S.M.K. Airaksinen, A.O.I. Krause, Ind. Eng. Chem. Res. 44 (2005) 3862.
[32] D. Tibiletti, F.C. Meunier, A. Goguet, D. Reid, R. Burch, M. Boaro, M. Vicario, A. Trovarelli, J. Catal. 244 (2006) 183.
[33] S. Ricote, G. Jacobs, M. Milling, Y. Ji, P.M. Patterson, B.H. Davis, Appl. Catal. A 303 (2006) 35.
[34] A. Goguet, F.C. Meunier, D. Tibiletti, J.P. Breen, R. Burch, J. Phys. Chem. B 108 (2004) 20240.